Magnetic Phase Transitions in Lattice Magnet Configurations Modelled by the 2D Ising Model and Monte-Carlo Markov Chain Algorithms.

PHY204 - Project 4

Andrey PILLAY[a], Ryan SFEILA[b], and Paul MATHIOT [c]

Abstract. Throughout this project, we investigate the properties and behaviors of simple magnetic systems using a 2D Ising model and stochastic computational methods. By simulating lattice configurations and incorporating notions from statistical physics and thermodynamics, we explore key concepts such as Curie's law of paramagnetism, spontaneous magnetization, and the lattice's response to external fields and temperature variations. We are particularly interested in recovering evidence of phase transition analogous to the predicted shift from paramagnetic to ferromagnetic character when nearing the Curie temperature of certain materials.

Key words: Paramagnetism, Ferromagnetism, Ising Model, Phase Transition, Magnetization, Magnetic Susceptibility, Curie-Weiss Law.

Contents

[a] e-mail: andrey.pillay@polytechnique.edu
[b] e-mail: ryan.sfeila@polytechnique.edu
[c] e-mail: paul.mathiot@polytechnique.edu

1 Introduction

The main goal of this project is to investigate and highlight *phase transitions* and other peculiar behavioral characteristics of a regular array of atoms that interact with each other and external magnetic fields as a result of their individual magnetic dipole moments induced by their atomic spin that is in one of two opposing states. To this end, we formalize our problem in the setting of a 2D Ising model. We elaborate below on both the relevant topics of physics regarding the unfolding of the project as well as the implications of our numerical implementation and simulation. Furthermore, we will extend the model to a continuous set of spin values and investigate how this affects the above mentioned effects.

1.1 Atoms as Magnetic Dipoles and Phase Transitions

We consider the magnetic aspect of matter. More specifically, as a consequence of the orbital and spin magnetic moments induced by an atom's electrons and nucleons, an atom bears a complex resultant magnetic moment. Depending on the material at hand, the atoms will bond differently, leading to different inter-particle interactions as well as different responses to applied stimuli, namely external magnetic fields. These characteristic behaviors depend on the number of unpaired electrons in the atomic orbitals and the relative states of electrons within interaction range. When studying a system of particles, we are interested in the resulting configuration under various conditions and transformations. This configuration depends on the material's characteristics, such as magnetic susceptibility and the effect of magnetization sites in conjunction with external magnetic fields. Two interesting classes of magnetic systems are paramagnetic and ferromagnetic systems, and the spirit of this project is to investigate the parameter regions in which a system undergoes a phase transition from the latter of these characteristic behaviors to the former while analyzing all the relevant quantities within and around this shift. Indeed, Curie's law predicts a certain scaling of a material's susceptibility with its absolute temperature. Furthermore, it predicts a singularity occurring at a critical temperature point below which materials start to spontaneously gain magnetization. This project also serves as a thorough exploration of what is meant by spontaneity, and the balance between thermal agitation and the stabilizing aspect of low-energy states.

1.2 The 2D Ising Model and Stochastic Numerical Methods on Lattice Configurations

Arising from the need to model the physics of phase transitions where a small change in a parameter such as pressure or temperature causes a significant macroscopic shift in character came the Ising model. This model derives from a mathematical problem formulated by physicist Wilhelm Lenz and proposed to his student Ernst Ising, who worked on it in the 1920s. In fact, it is possible to treat the entire problem without considering any physical interpretation of magnetic systems, which is only proof of the powerful yield of this problem, which is yet to be solved in dimensions higher than 2 (Cipra 1987[1].) In our project's setting, we consider a two-dimensional square array called a lattice, and each position along the rows and columns of this array constitutes a lattice site that takes one of two states, that we use to represent the atoms. Briefly, the idea is to run a simulation that uses the governing physical laws to create an evolution of the lattice configurations. We undertake this process probabilistically to mitigate very computationally expensive tasks; this is a very interesting aspect of the project and the methods are thoroughly outlined in the subsequent sections of this report along with our methodology for extracting the measurements of physical quantities. The simplistic formalization of such a complex problem rooted in quantum mechanics is very exciting, but it also demands an important awareness and analysis of the scope of validity as a demonstration of natural phenomena; it is important to remember the physical purposes of such numerical methods. Up to our approximations and estimations, the 2D Ising model does indeed recover - to an extent - the phase transitions proved by Onsager's impressive analytic solution to the problem and the existence of the discontinuous point that is the Curie temperature with regards to magnetization evolution. Interesting questions for future exploration could revolve around extending the scope of validity of the model to the specific problem of modeling thin film ferromagnets, but also to study the Ising model in different contexts as its notions extend to fields such as ML - Boltzmann machines and Hopfield networks - and lattice gas representation in statistical mechanics.

2 Theoretical background

We dedicate this section to outlining the essential preliminary, theoretical background required to give an enhanced contextualization of the problem and understanding of the manner in which the project tasks were undertaken. The theoretical information in question revolves around the following:

- The Ising model setup.
- Notions from statistical mechanics.
- Stochastic integration and the MCMC method.
- Paramagnetism, ferromagnetism, and diamagnetism.
- The Curie-Weiss law.
- Measurables, the free energy, and spontaneity.

2.1 Positioning the Problem

Consider a two-dimensional, square lattice structure containing $N = L \times L$ lattice sites, each bearing a state $\sigma_i \in \{-1, 1\}$. This refers to the magnetization state of the lattice site, which, in a physical setting, could refer to an atomic spin. We call the configuration

$$\sigma = (\sigma_1, ..., \sigma_N) \in \{-1, 1\}^N$$

the full description of the lattice state - parametrized by the individual magnetization states of the lattice sites - at a given instant. We are interested in finding the configuration of the system upon imposing certain parameters such as temperature. Hence, we must establish how to choose valid, or favorable, states depending on the system parameters. We have two clashing effects at hand:

- The energy of a configuration.
- The thermal agitation of the system.

We combine these effects in an interesting function derived from statistical physics. But first, we need the extraction of an energy from a configuration due to interactions.

2.1.1 The Hamiltonian

To this end, we consider the Hamiltonian application on a configuration which yields its energy and which is defined in this problem as:

$$\mathcal{H} : \begin{cases} \{-1,1\}^N & \longrightarrow \mathbb{R} \\ \sigma & \longmapsto \mathcal{H}(\sigma) = -E \sum_{<i,j>} \sigma_i \sigma_j \; - \; J \sum_{i=1}^{N} h_i \sigma_i \end{cases}$$

In the above definition of $\mathcal{H}$, the parameters are defined as stated below:

- The family $(\sigma_i)_i$ refer to the lattice sites defining $\sigma \in \{-1,1\}^N$.
- The notation $< i,j >$ refers to immediate neighbors; the model includes the implicit assumption that a lattice site only interacts (at least in a non-negligible fashion) with its direct neighbors. The model also includes the "wrap-around" approximation which should, in principle, marginally affect our results. (We would have liked to model an infinite lattice, but we instead assume the leftmost (or highest) lattice site interacts with the rightmost (or lowest) site.)
- The parameters E and J define the interaction characteristics of the lattice; the parameter E determines how much two neighborinh lattice sites interact, and whether parallel/antiparallel spins are more/less energetic states, while the J parameter determines the interaction of a lattice site with the external field.
- The family $(h_i)_{1 \leq i \leq N}$ quantifies the external field applied on a given lattice site. In all of the subsequent demonstrations, we will set these parameters to 1. This represents a uniform external magnetic field in the "up" direction.

Hence, we can look at the energy as the sum of the inter-particle interaction energies and the sum of the particle interaction energies with the external, applied magnetic field.

2.1.2 The Partition Function

We can now combine this interaction energy with thermal agitation and determine which states are "favorable". Consider the partition function defined as the following sum over all possible configurations of the lattice sites in the $N-$sized lattice:

$$Z : \begin{cases} \mathbb{R}_{>0} & \longrightarrow \mathbb{R} \\ T & \longmapsto \sum_{\sigma \in \{-1,1\}^N} \; e^{-\frac{1}{k_B \, T} \, \mathcal{H}(\sigma)} \end{cases}$$

We make the following observations:

- Both the Hamiltonian and the partition function (implicitly) depend on E, J, and $(h_i)_i$.
- The parameters T and k_B respectively denote the absolute temperature of the system and Boltzmann's constant (which relates temperature to kinetic energy.)
- It goes without saying that Z is a function of N, the lattice size, but this parameter is only initialized so we do not consider it as a function argument (but instead a setting defined before the partition function definition for our model.)

Observe that in this formalism, we can only probabilistically determine favorable states (similar to QM.) The probability of a configuration manifesting under given temperature and interaction parameter conditions is given by:

$$\mathbb{P}(\sigma) = \frac{1}{Z(T)} \, e^{-\frac{1}{k_B \, T} \, \mathcal{H}(\sigma)}$$

We quickly observe that, for instance, under fixed temperatures, lower energy configurations are favorable. We can also observe that, at very high temperatures, there is little favorability attributed to lower energy configurations, and state sampling becomes closer to uniform.

From the probability of a configuration, we deduce that, all parameters fixed, lower energy states are more favorable. Consequently, from the Hamiltonian's form and if $E > 0$, we deduce that neighboring

lattice sites with parallel spins are more favorable, and we expect regions of aligned spins throughout the lattice in the absence of an external field. Similarly, considering all sites experience the same field, we expect that upon introduction of a strong enough external field, then sites all align along or against the external field depending on the sign of J. The signs and magnitudes of E and J depend on the type of material (unpaired electrons,...) Most materials can be classified as either *diamagnets*, *ferromagnets*, or *paramagnets*.

- *Diamagnets* tend to slightly oppose applied fields and exhibit zero dipole moments per atom; they have paired electrons.
- *Paramagnets* have unpaired electrons and slightly align with external fields.
- *Ferromagnets* have high magnetic susceptibility and exhibit spontaneous magnetization. This doesn't translate directly to a strong magnetic field, however, as the material is typically divided in distinct regions called Weiss domains, within which the spins are aligned but not necessarily with other domains. As such, the field originating from different regions cancels out and the overall net magnetic field is weak.

Throughout this project, we are particularly interested in paramagnetic and ferromagnetic behaviors, which, as we will see, depend on temperature. Observe that increases in temperature attenuate the differences in the probability of the different states, making disordered states relatively more favorable than they were at lower energies. We will examine this behavior in the subsequent sections of this project.

2.2 A Brief Introduction to the MCMC Method

The main problem with this probabilistic setup is the difficulty of computing the partition function at very large N - it involves a very large summation. We do not elaborate too much on the specifics of the numerical implementation required to demonstrate the evolution of configurations following the probability distribution defined by the partition function; this is outlined in Appendix A. The general idea is that we can a Markov chain structure and relative configuration probabilities to sample configurations following the desired law (under uninteresting conditions outlined in said appendix.) We then take advantage of statistical limit theorems to estimate the theoretical expectation of the random variables that are the system's physical quantities and characteristics.

2.3 Physical Quantities and Phenomena in the Ising Model

In this setting and within this framework, we can consequently and precisely talk about what we intend to achieve with this Ising model. Very roughly speaking, we want to extract physical quantities and data in a computationally efficient manner and ideally recover the phase transition and physical phenomena predicted by results in the literature.

2.3.1 Magnetization

Consider the slightly simpler form of the Hamiltonian, where all lattice sites are exposed to the same external field:

$$\mathcal{H}(\sigma) = -E \sum_{<i,j>} \sigma_i \sigma_j \; - \; J \sum_{i=1}^{N} \sigma_i$$

Then recall that infamous partition function where $\beta := (k_B T)^{-1}$:

$$Z : \begin{cases} \mathbb{R}_{>0} & \longrightarrow \mathbb{R} \\ T & \longmapsto \displaystyle\sum_{\sigma \in \{-1,1\}^N} e^{-\beta \, \mathcal{H}(\sigma)} \end{cases}$$

The average magnetization of the lattice is defined by the following function:

$$\langle M \rangle : \begin{cases} \mathbb{R}_{>0} & \longrightarrow \mathbb{R} \\ T & \longmapsto \frac{1}{\beta} \frac{\partial}{\partial J} \ln Z \end{cases}$$

where J refers to the J parameter in the Hamiltonian.

Now, to compute this quantity in our experiment without the expensive computation of Z, it can be shown that the average magnetization writes as

$$\langle M \rangle = \mathbb{E}\left[\sum_i^N \sigma_i\right],$$

the explicit derivation of which is found in Equation 1.

Then, for some fixed system parameters, suppose we store K sampled configurations using our MCMC algorithm under the assumption of a stationary probability distribution in our Markov Chain (enough warmup) and an adapted cycle length (Monte-Carlo steps between measurements) to avoid sampling correlated configurations, one can check that by the established principles of importance sampling and the MCMC algorithm in question, an averaging of the empirical values of $\sum_i^N \sigma_i$ over our Monte-Carlo configurations should indeed converge to the full integral or the true magnetization. Computing expectations are, after all, at the heart of stochastic integration and MCMC algorithms.

Naturally, we expect that, upon removing the external field, we retrieve the random states with net 0 magnetization. This is true above a certain temperature, but we observe spontaneous (or residual) magnetization below said temperature, i.e. a relatively ordered state is spontaneously achieved. This is one illustration of a phase transition (magnetization in the absence of applied field.) All ferromagnets behave as paramagnets above a certain temperature, that we call the Curie temperature of the material. As for why this spontaneous process occurs, we explain it briefly in a later section dedicated to Helmholtz Free Energy.

We might be interested in taking our measurements to the thermodynamic limit - that is when $N \to +\infty$. Hence, it may be more relevant to average the magnetization over the lattice size to get the average magnetization per lattice site, which amounts to adding a $1/N$ factor in the expectation and in the expression of the magnetization:

$$\langle m \rangle : \begin{cases} \mathbb{R}_{>0} & \longrightarrow \mathbb{R} \\ T & \longmapsto \frac{1}{N\beta}\frac{\partial}{\partial J} \ln Z \end{cases}$$

The following follows immediately:

$$\langle m \rangle = \mathbb{E}\left[\frac{1}{N}\sum_i^N \sigma_i\right]$$

2.3.2 The Magnetic Susceptibility

The magnetic susceptibility of the system is defined as:

$$\chi : \begin{cases} \mathbb{R}_{>0} & \longrightarrow \mathbb{R} \\ T & \longmapsto \frac{\partial \langle m \rangle}{\partial J} = \frac{1}{N\beta}\frac{\partial^2}{\partial J^2} \ln Z \end{cases}$$

Following the computation in Equation 2, we can write (where β is obviously a T dependent function):

$$\chi(T) = N\beta \text{ Var } \left[\frac{1}{N}\sum_{i=1}^N \sigma_i\right] = N\beta(\langle m^2 \rangle - \langle m \rangle^2)$$

Note that we are treating the measurables as random variables with probability distributions dictated by the partition function. and estimate them with realizations of their empirical mean, a good approach justified by statistical limit theorems.

Magnetic susceptibility is a measure of how readily a system aligns its net magnetic moment with an applied external field. From Jensen's inequality, the magnetic susceptibility should not change sign (it does not have to be positive depending on the sign convention in the Hamiltonian.) We will investigate a certain scaling law predicting a singularity of χ at the Curie temperature T_C before an expected sign change, where the susceptibility is no longer properly defined. This singularity denotes the point of phase transition that we seek. Once again, the tendency of the system to respond to applied fields in certain ways is related to the system's free energy evolution under temperature and external field variation.

2.3.3 The Internal Energy

The system's average internal energy is given by:

$$\langle E \rangle : \begin{cases} \mathbb{R}_{>0} & \longrightarrow \mathbb{R} \\ T & \longmapsto -\frac{\partial}{\partial \beta} \ln Z \end{cases}$$

The lattice's energy is the weighted average of the possible configurations' energies (Hamiltonian application) - weighted by their probabilities. Computations in Equation 3 yield:

$$\langle E \rangle = \mathbb{E}[\mathcal{H}(\sigma)]$$

2.3.4 The Heat Capacity

The definition of the heat capacity with respect to the energy is analogous to that of the magnetic susceptibility with respect to the magnetization. The lattice's heat capacity (denoted as an isochoric heat capacity seeing as we don't incorporate size changes) can be interpreted as the system's "susceptibility of storing energy as internal, potential energy rather than vibrational kinetic energy". Another interpretation is the energy required to force an increase in temperature. It is defined in terms of the partition function as follows:

$$C_V : \begin{cases} \mathbb{R}_{>0} & \longrightarrow \mathbb{R} \\ T & \longmapsto \frac{\partial \langle E \rangle}{\partial T} = \frac{\partial}{\partial T}\left(-\frac{\partial}{\partial \beta} \ln Z\right) \end{cases}$$

Once again, to adapt the computation to our simulation, Equation 4 demonstrates:

$$C_V(T) = \beta^2 k_B \text{ Var } [\mathcal{H}(\sigma)] = \beta^2 k_B (\langle E^2 \rangle - \langle E^2 \rangle)$$

2.3.5 The Free Energy and the Thermodynamic Limit

Finally, arguably the most interesting physical quantity of our system is the free energy. The main purpose of mentioning it here is to understand our system's evolution and how phase transitions were predicted or analytically sought in the historical context of the Ising model problem. The equilibrium free energy per lattice site of the system is given by:

$$\mathcal{F} : \begin{cases} \mathbb{R}_{>0} \times \mathbb{R} \times \mathbb{R} & \longrightarrow \mathbb{R} \\ (\beta, E, J) & \longmapsto \lim\limits_{N \to +\infty} \frac{1}{N\beta} \ln Z(\beta, E, J) \end{cases}$$

Very roughly speaking, the free energy function balances the two clashing effects we had previously mentioned - lower energy levels and thermal agitation. A better interpretation of the free energy is the weight of the following effects on the equilibrium state a given instant:

- Lower energy states are more probable/favorable/stable.
- The system naturally tends to more disordered states (of higher entropy), and increases in entropy are more stabilizing at very high temperatures.

We take the thermodynamic limit because that is where these principles are physically relevant, and this explains our attempts at eliminating the free boundary effect in our finite model by introducing a "wrap-around" in our lattice.

The general form of the Helmholtz free energy of a system in a given configuration is the following, where U is the internal energy of the system, S is the entropy, and T is the absolute temperature:

$$F = U - TS.$$

Processes are spontaneous when the final free energy of the process is lower than the starting one; systems tend to configurations with lower free energies, and the sign of the change in free energy depends on the system's configuration (more specifically, its Hamiltonian return value/internal energy.) Furthermore, it depends on the change in entropy, and this is weighted with the absolute temperature of the system.

Hence, when speaking about phase transitions of the Ising model, we are referring to the discontinuities we expect in the solution $\mathcal{F}$ to our Ising model; discontinuities in the equilibrium free energy foreshadow the existence of several equilibrium states for a given set of parameters, singularities in quantities, and hence the phase transitions under certain transformation and the possibility for hysteresis cycles, which would not be possible for continuous functions that map parameters to well-defined values.

We make a final interesting observation. Had we not taken the thermodynamic limit, we would not be able to expect singularities or discontinuities as the free energy function is an analytic, well-defined, continuous function of the state, and we would not observe well-pronounced phase transitions, which strongly encourages us to include this "wrap-around" effect. Even now, as we will observe, we do not observe absolute singularities because of the finite model effect, but we do recover similar patterns.

2.4 Curie's Law

Curie's law connects the magnetic susceptibility of a paramagnetic material with its temperature. It states that for a fixed value of the external field, the susceptibility is inversely proportional to the temperature, i.e.:

$$\chi = \frac{C}{T}.$$

The law's derivation is available in the PHY204 Textbook [3] but also appears in a very insightful lecture by Leo Radzihovsky[2] on exact solutions to magnetism problems and the Ising model.

For ferromagnetic materials, this law can be specified in the form known as the Curie-Weiss law, which states that in their paramagnetic state (hence for $T > T_C$), we have the inverse proportionality:

$$\chi = \frac{C}{T - T_C}.$$

We see that this law predicts a singularity of the susceptibility at the critical temperature. This will be used as an indicator in the numerical simulation to determine T_C experimentally.

2.5 The Hyperbolic Tangent Scaling of the Magnetization

Curie's law is very appealing, but it only applies well at high temperatures and low susceptibilities as demonstrations reveal. A more general scaling law is also derived in [3] and writes as

$$\chi = \mu_B \tanh\left(\frac{\mu_B B}{k_B T}\right)$$

The hyperbolic function hints at a combinatorial manipulation of the terms of the portion function before differentiation to obtain the magnetic susceptibility. with B the magnitude of the field and μ_B Bohr's magneton. In our simulation, we will simply write $\mu_B = 1$. We recover from this expression that for big temperatures, the fraction inside the tanh becomes small, and as such we can approximate $\tanh(x) \sim x$, and we recover the previously presented Curie's law.

2.6 Hysteresis

The phenomenon of hysteresis can be encountered when an external magnetic field is applied to a ferromagnetic material. It describes the fact that for a given value of the imposed field, we can not determine in which state the material is, i.e. the magnetization can take multiple values for a given external field. To explain this phenomenon, let us recall that in a ferromagnetic material not subject to an external field, we observe the Weiss domains. These are regions where inside the domains the spins are aligned. When we introduce a field, the spins tend to align themselves with it, leading to more Weiss domains being oriented with the magnetic field. When we keep on increasing the magnitude of the field, more and more domains align themselves until saturation is reached – all the spins are aligned. Once this state is reached, the material is permanently magnetized. The ferromagnetic interaction between the spins ensures that the magnetization will be preserved even when the field is removed. We need an additional field in the opposite direction to reduce the magnetization. The same process can then be repeated in the other direction and we see that, for example, in the absence of a field, we could have a magnetization in both directions, implying that the history of the material is necessary to determine its state. The non-zero magnetization in the absence of an external field (after saturation) is called the saturation remanence, and the magnitude of the field needed to change the magnetization is the coercivity of the material.

2.7 Importance of the Ising Model to Simulate Ferromagnetism

As mentioned above, we demonstrate the phenomenon of phase transition and provide interpretations of the simulation as an analogy of a thin film para/ferro - magnet. The concept of spontaneous magnetization allows us to understand how materials with high Curie temperatures can be forced to bear very high magnetization states permanently. The exploitation of stable, nonzero magnetization states has important applications and we list two below:

- Hard Drive Disks: Controlling the state of magnetic domains on HDDs allows us to store, read, and write data to/from the magnetic domains of the storage site.

- Magnetoresistive Random Access Memory (MRAM): MRAM exploits the magnetic phase transitions in materials where electron spin is used, along with charge, to store data. The transition between magnetic states in magnetic tunnel junctions (MTJs) is used to represent different data states. Unlike conventional RAM, MRAM retains data without power, thanks to the stability of the magnetic phase transitions.

Other applications include MRI imaging, permanent magnetic creation in automobile components, and even spintronic devices for advanced computing and magnetic tunnel junctions. These are the applications of results for a magnetic system, but more applications of the mathematical formulation of the Ising model can be found in Appendix D.

3 Simulation method

In this section, we will look at the numerical implementation of the model described above. The detailed implementation of said algorithms is available in the provided python file.

3.1 A Small, Preliminary Note on Parameter Scale

An important limitation of our simulation is the floating point error created by the very small Boltzmann constant, which we've consequently reset to 1. All this means for our model is that the temperature inputs must be assumed to be linear transformations of the absolute temperature (multiplication by a small positive number.)

This is not very damaging to our experiment as we are far more interested in the relative fluctuations and the overall trend rather than specific values in S.I. units.

3.2 First Implementation: Discrete Spins

In this first implementation, we intend to model the behavior of paramagnetic and ferromagnetic materials. To do so, we implemented numerically the classical Ising model in two dimensions. We consider a lattice of size $N = L \times L$, where each node (i, j) of the lattice contains a spin $\sigma_{i,j}$ with values in $\{\pm 1\}$.

There are two simplifications we made when creating our model. First of all, our lattice "wraps around", meaning that the left and right boundaries coincide as well as the top and bottom. This amounts to working with coordinates modulo L. The second simplification is the assumption that it is enough to consider only interaction from one spin to its direct neighbors and neglect other possible interactions.

We modeled the lattice in a class `Configuration`. It is equipped with methods to compute the magnetization and the Hamiltonian of the system.

Additionally, the class accepts multiple input arguments and disposes of numerous methods allowing us to perform a strong diagnostics for a wide variety of settings.

We implemented the evolution of the system using the Metropolis-Monte-Carlo algorithm: we start by sampling a location (i, j) of the lattice and compute the energy difference associated to flipping the spin $\sigma_{i,j}$ at this location using the formula

$$\Delta\mathcal{H} = 2(E\sigma_{i,j}(\sigma_{i-1,j} + \sigma_{i+1,j} + \sigma_{i,j-1} + \sigma_{i,j+1}) + Jh_{i,j}\sigma_{i,j}).$$

To this energy difference, we associate an acceptance probability $p(\Delta\mathcal{H})$, that scales as an exponential $p \sim e^{-\beta\Delta\mathcal{H}}$. This probability determines if the proposed change of the spin should be accepted. A step in the evolution of the configuration then consists of repeating this simple Monte-Carlo step a number

of times. In our case, we propose N changes per simulation step. This ensures that two consequent configurations are not correlated.

For the later analysis, we require information on the different physical quantities of the system. Considering the stochastic nature of our simulation, it only makes sense to consider "temporal" average of each measurable. Note that what we consider time as steps of the MMC, and not the physical flow of time.

To compute these averages, we first run the simulation for a certain number of steps, the "warm-up" time, so that an equilibrium configuration is attained. Once this is done, we measure the desired quantity on configurations, for a certain number of collection steps. We then compute the average of these measured values. Following this procedure, we can measure the following quantities:

- The magnetization $\langle m \rangle$, which is the sum of the spin divided by the lattice size N:

$$\langle m \rangle = \frac{1}{L^2} \sum_{1 \leq i,j \leq L} \sigma_{i,j}.$$

- The energy $\langle e \rangle$, which is given by the Hamiltonian indicated above.
- The magnetic susceptibility χ, which is proportional to the variance of the magnetization:

$$\chi = \beta L^2 (\langle m^2 \rangle - \langle m \rangle^2).$$

- The heat capacity c_v which is proportional to the variance of the energy:

$$c_v = \beta^2 L^2 k_B (\langle e^2 \rangle - \langle e \rangle^2).$$

To interact with the simulation, we wrote a function that displays the lattice with colors according to the orientation of the spin. We also made it possible to change the temperature and the magnitude of the external magnetic field (that has a constant "up" direction) as the simulation is running. Additionally, we actively plot the magnetisation and the energy of the configuration. This allows us to have a direct visual feedback of the effect at hand. A screenshot of the result can be found in Figure 1.

3.3 Second Implementation: Continuous Spin Distribution

For the second part of the numerical aspect of this project, we looked at a lattice where the spins are now allowed to have an arbitrary direction (in the plane). To implement this, we attributed to each node (i, j) on the lattice, a value $\sigma_{i,j}$ in the interval $[-1, 1]$, which corresponds to the angle with the vertical axis (up to normalization.) A value of 0 corresponds to a spin pointing upwards, 0.5 pointing left, etc.

To compute the new Hamiltonian of the system, we can use the same formula as before, but replace the multiplication of the spins by the dot product of neighboring spins. As every spin is normalized, this amounts to the cosine of the difference between their respective orientation. A similar reasoning induces that the magnetic part of the Hamiltonian is replaced by the dot product of the magnetic field direction with the spin at each lattice point.

$$\mathcal{H} = -E \sum_{<i,j>} \cos(\pi(\sigma_i - \sigma_j)) - J \sum_i \cos(h_i - \sigma_i)$$

The simulation of the system then follows the same steps as in the discrete case. We sample a location (i, j) on the lattice and choose a new orientation of the spin $\sigma_{new} \in [-1, 1]$. We then compute the acceptance probability using the energy difference, taking into account that it now writes as a sum of cosines.

The acquisition procedure is the same as for the discrete case, but we have to take into consideration that the magnetization is now a vectorial quantity. We compute it by summing (as vectors) all the moments of the lattice and dividing the results by the size N of the lattice.

To visualize the simulation, we wrote another method to display the lattice with colors according to the orientation of the spins. To achieve this, we mapped the orientation on the unit circle on the following gradient. For additional clarity, we added arrows indicating the direction of the magnetic moment at every point. Finally, since the magnetization is now a vector, we plot its magnitude as well as its orientation in parallel of the visualisation. A screenshot of the result can be found in Figure 2.

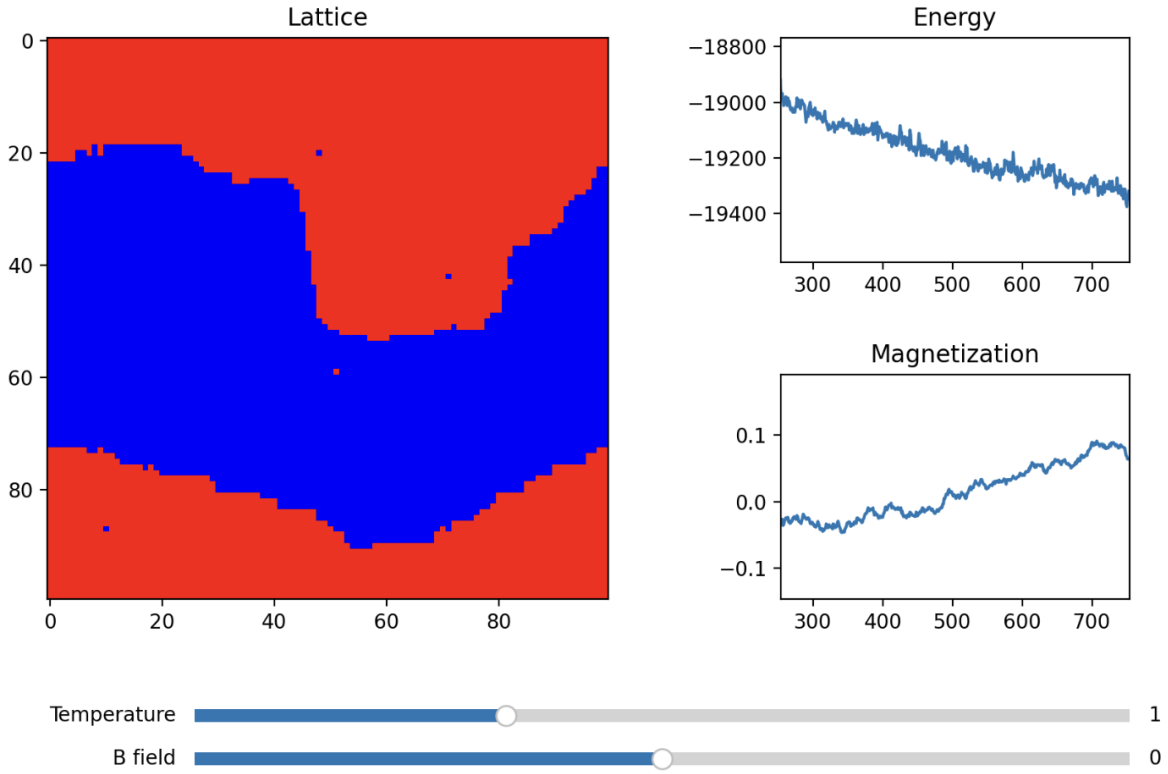

Fig. 1: Visualization of the simulation in the discrete case

4 Results and Discussion

4.1 Preliminary Observations

To assess if our implementation accurately models the desired system, we start with simple observations made on the visualisation we made.

1. The first and simplest observation is the dependency on the temperature of the system. These are done in the absence of an external magnetic field. We expect the system to exhibit two types of behaviors depending on the value of the temperature. For high temperatures, we expect the orientation of the spins to random, due to the thermal agitation. This is indeed what we observe. When we look at low temperatures, we expect the interaction between neighboring spins to dominate against the thermal agitation and as such, we expect to observe the so-called Weiss domains, regions in the lattice where the spins align themselves. Once again we observe with our simulation exactly the expected behaviour. We also observe that the constant E influences the threshold between the two behaviours. Some illuminating examples can be observed in Figure 3.
2. The second effect we can observe regards the introduction of the magnetic field. We expect the spins to align themselves when subject to an external field, with the direction of orientation being dictated by the direction of the field. Using our simulation, we confirm these expectations, which hints towards a correct implementation of the external field. The examples can be seen in Figure 4

4.2 Phase change

Let us now analyse our simulation further and identify that it replicates the phase change we expect when the temperature drops below the critical temperature. We will furthermore experimentally determine this temperature and compare it to the theoretically expected one.

To display the phase change, we ran the simulation on a set lattice size $L = 50$ and measured the average magnetization, energy, susceptibility, and heat capacity for increasing temperatures, see Figure 5.

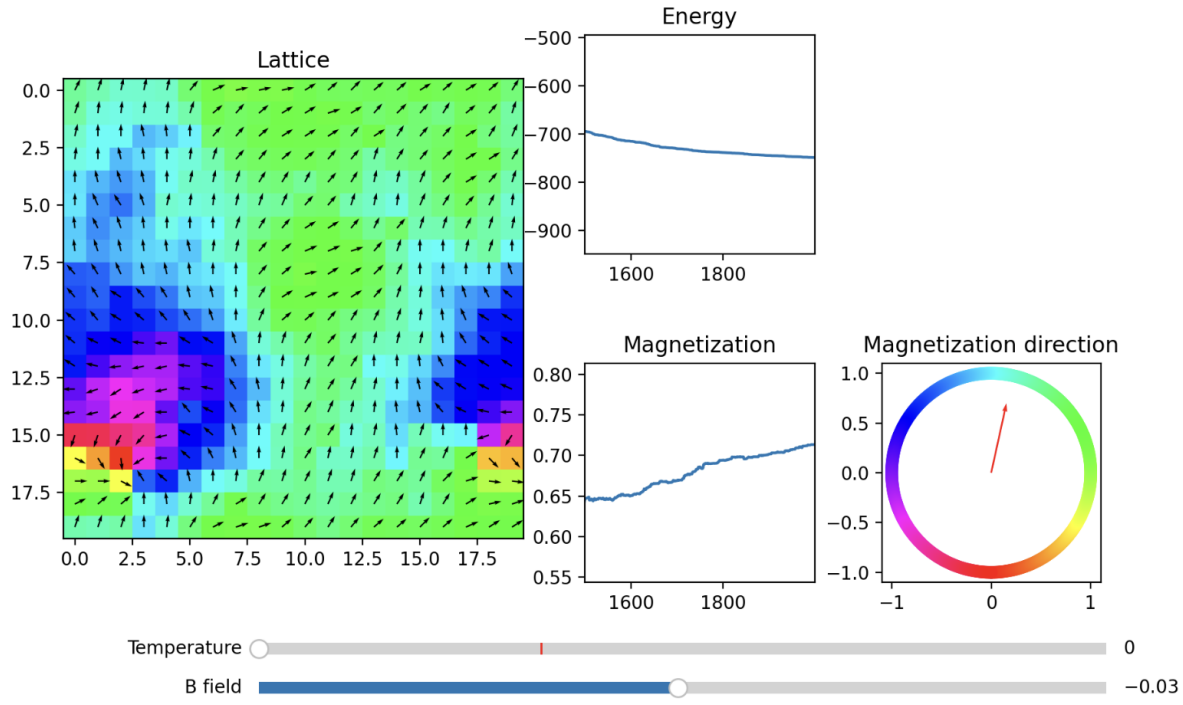

Fig. 2: Visualization of the simulation in the continuous case

Following the theory presented above, we see that the expected behavior around the critical temperature T_C is retrieved. By definition, the critical temperature is the one for which the magnetization suddenly drops. In addition to a drop of magnetization, we expect the energy to strongly increase around T_C. Indeed, when transitioning we go from an ordered state with a very low energy to a disordered random state, that has high energy. As seen in earlier parts of the report, we also expect the susceptibility to peak at the critical temperature, as predicted by Curie-Weiss. Finally, the heat capacity is proportional to the variance of the energy. As such, we expect it to be highest when the energy is strongly varying, meaning around the critical temperature T_C. As seen in the graph, all four of these indicators are observed for our numerical simulation, thus confirming that we observe the desired phase transition.

A quick analysis of the different quantities presented in Figure 6, Figure 7 and Figure 8 gives us an experimental value of $T_C \approx 2.34$, which fits nicely with the theoretically expected value $T_{C,th} \approx 2.27$.

4.3 Curie-Weiss law

Another behavior we wish to confirm with our simulation is the Curie-Weiss Law.
Plotting the inverse of the magnetic susceptibility of our lattice against the temperature, we get Figure 9. Note that we consider temperatures above the critical temperature and that we are working in the absence of an external magnetic field. We see that we retrieve the expected linear relationship:

$$\chi = \frac{C}{T} \iff \frac{1}{\chi} = \frac{1}{C}T - \frac{T_C}{C}$$

with C a material-dependent constant called the Curie constant.
A linear fit of our data gives us the coefficients $a = \frac{1}{C} = 0.7, b = -\frac{T_C}{C} = -1.64$. We compute from those $C = \frac{1}{a} = 1.43$. This gives us another approximate of the critical temperature:

$$T_C = -bC \approx 2.34$$

We see that we recover the same critical temperature as the one determined already in subsection 4.2.

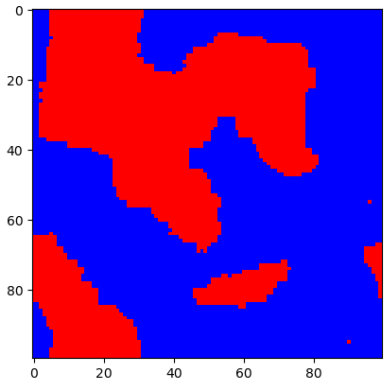

(a) $E = 1, T = 1$

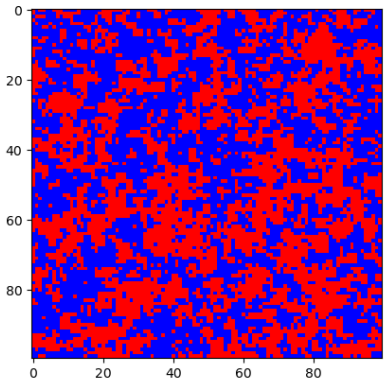

(b) $E = 1, T = 3$

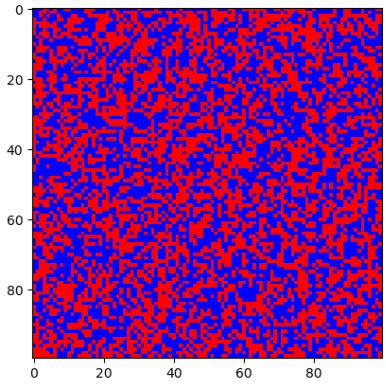

(c) $E = 0.1, T = 1$

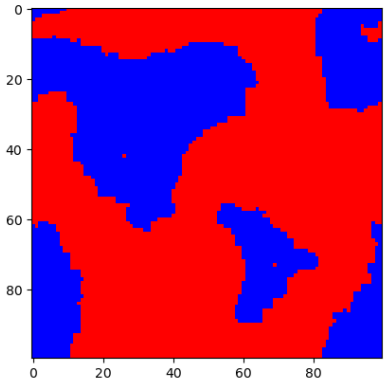

(d) $E = 0.1, T = 0.1$

Fig. 3: Examples of configuration (after some time passed) for different values of E and T

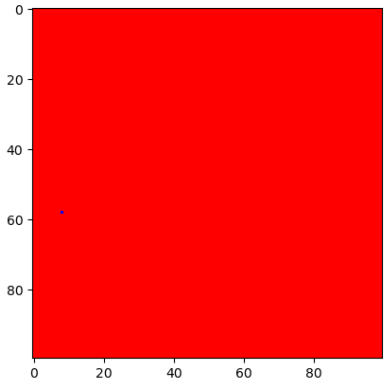

(a) $J = 1$

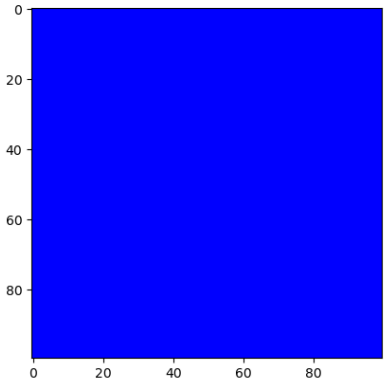

(b) $J = -1$

Fig. 4: Examples of configuration (after some time passed) for different values of J

4.4 Scaling of the magnetization

Another scaling law we can confirm is the one determining the behavior of the magnetization of a paramagnetic material subject to an external magnetic field.

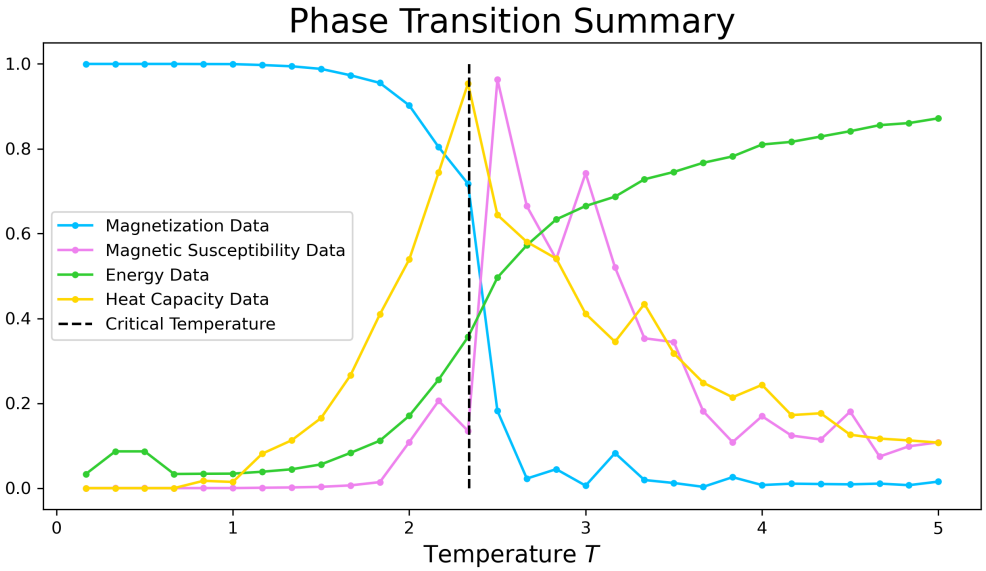

Fig. 5: Plot of the different measurables for $L = 50$

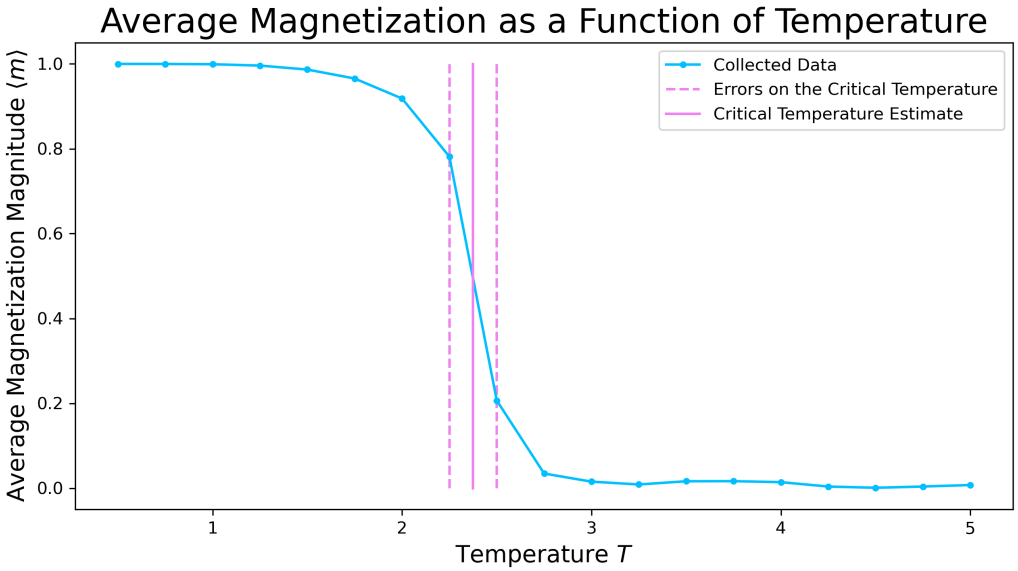

Fig. 6: $m - T$ diagram

To do so, we ran our simulation at a fixed temperature T, and recorded the magnetization for different values of the external field J. This resulted in the plot Figure 10. We fitted in this plot the theoretically predicted dependency:

$$\langle m \rangle = \tanh\left(\frac{\mu_B J}{k_B T}\right)$$

We see that our data matches the theoretical one extremely well. This shows that we succeeded in implementing the external magnetic field correctly.

4.5 Hysteresis

To observe hysteresis, we start with a configuration that is at equilibrium in the presence of an external magnetic field (in our case $J = +2$). We then decrease the magnitude of the magnetic field, until it flips

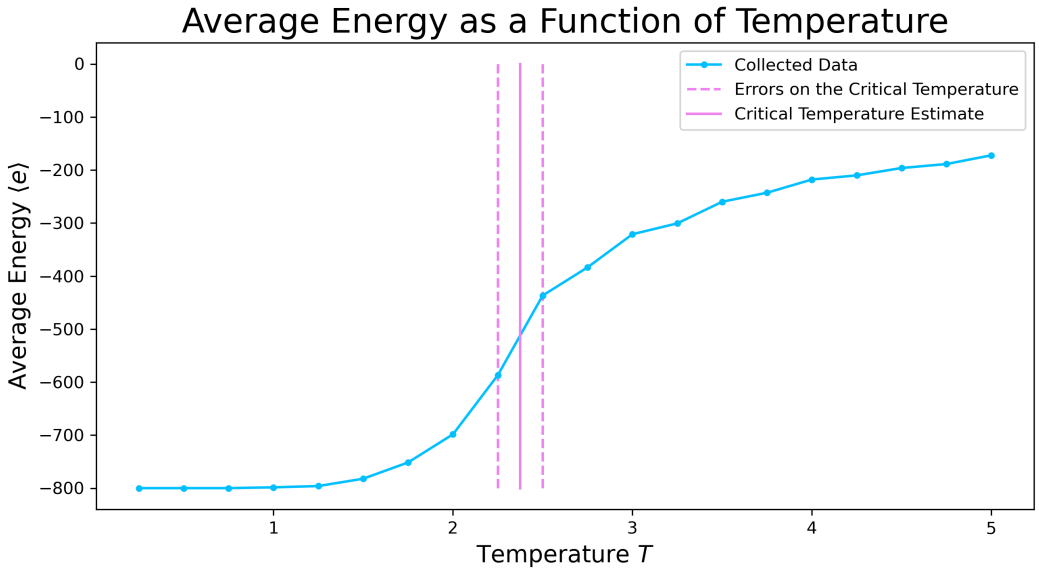

Fig. 7: $e - T$ diagram

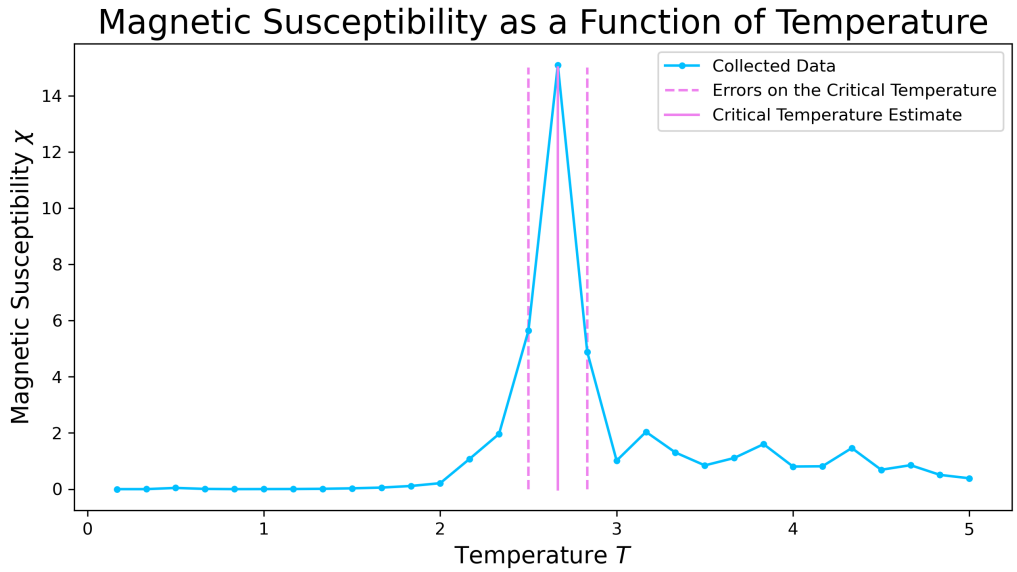

Fig. 8: $\chi - T$ diagram

sign and reaches a value of $J = -2$. As we do so, we record the magnetization of the lattice. We then let the configuration settle until equilibrium under a constant field. Once this is done, we increase the magnitude again until it reaches its initial value.
The plot resulting from this procedure can be seen in Figure 11. We observe clearly the multi-valuedness of the magnetization for a given value of the external field. The fact that the lattice conserves a non-zero magnetization when the field is brought back to zero confirms the expected non-linear behavior of the hysteresis, as presented in subsection 2.6. The coercivity measured in the frame of our simulation is of around 1.25 Oe.

4.6 The continuous case

The same analysis done for the discrete spin distribution can be done in the presence of continuous spins. Let us start with our preliminary observations. This is merely an attempt at showing the numerical

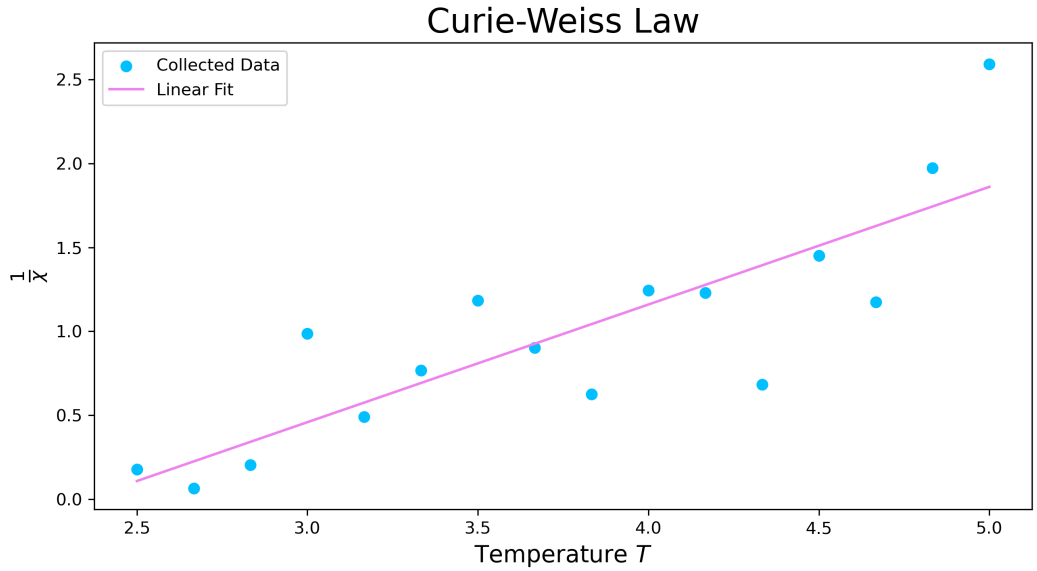

Fig. 9: Curie-Weiss law in the discrete case with $L = 50$

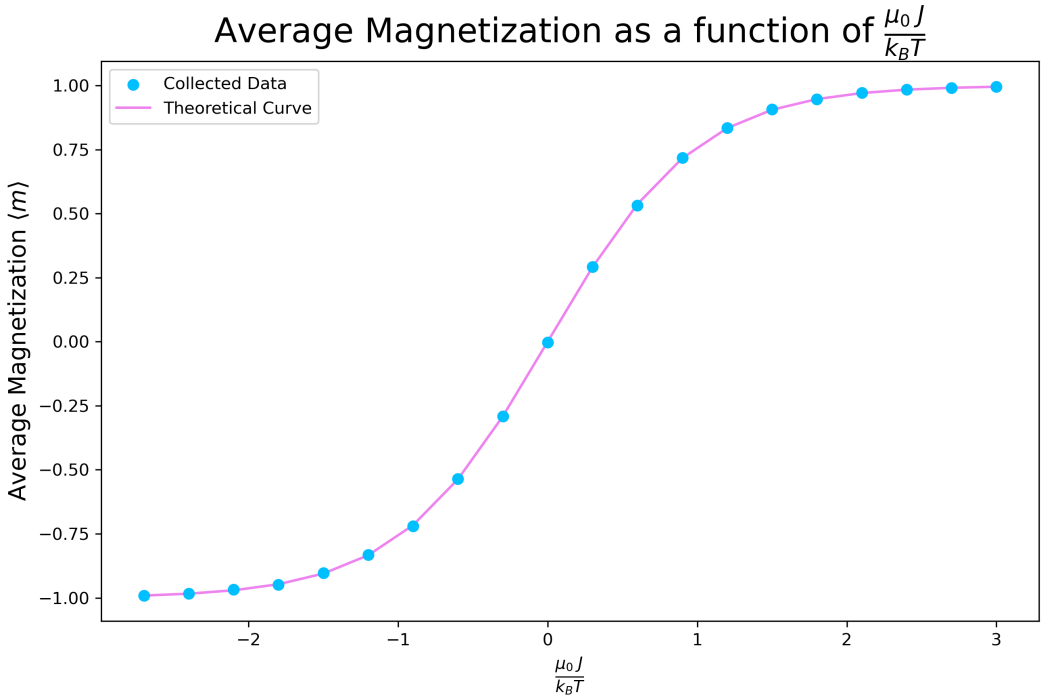

Fig. 10: Average magnetization plotted against the factor $\frac{\mu_B J}{k_B T}$ obtained by varying the magnetic field intensity

maneuverability of the Ising model and frameworks to solve other problems. A paper of its own would have to be dedicated to discussing the physical analog of what this continuum of states could represent. A good guess is a molecular compound, in which we have an array of molecules with net dipole moments resulting from their molecular geometry (an area where one could consider VSEPR theory isomers in interesting scenarios.)

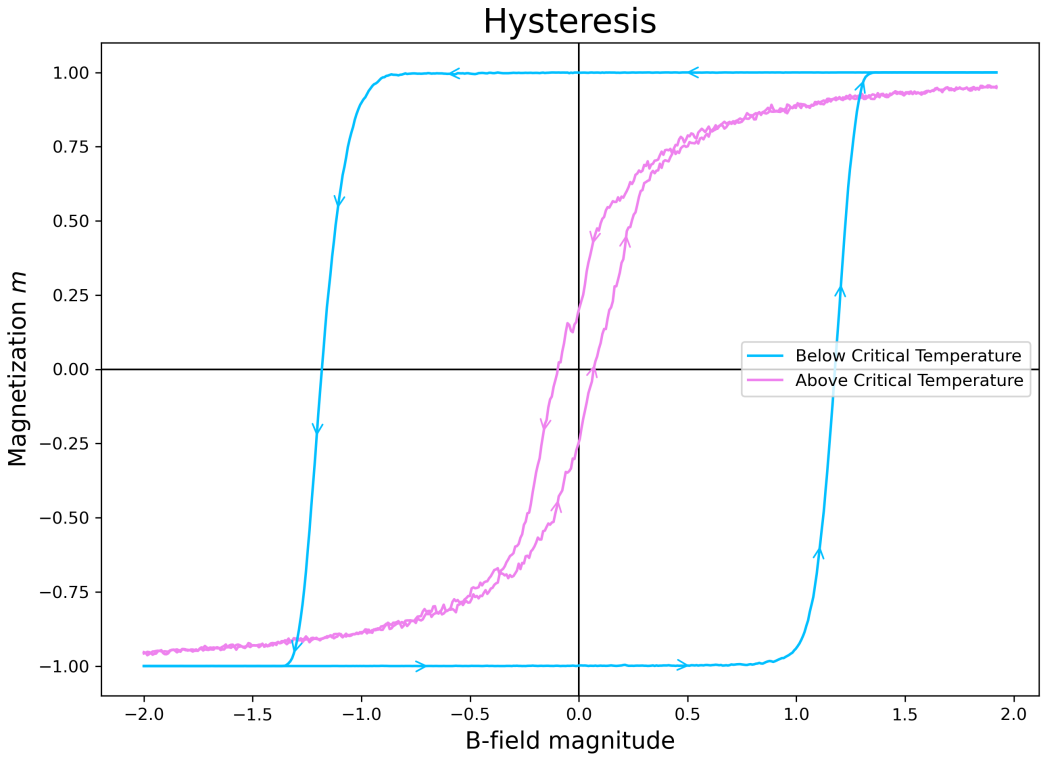

Fig. 11: Graph of the magnetization against the magnetic field over one cycle

4.6.1 Observations

1. Similarly to the discrete case, we observe again that the behavior of the system depends on the temperature. For high temperatures, we observe a random spin distribution, whilst for lower temperatures the spins tend to align themselves in Weiss domains. Since the spins can be oriented arbitrarily, we observe that the orientation of the spins in a specific domain is not constrained, meaning that we encounter domains with different orientations in the same lattice.
2. We also confirm the effect of the external magnetic field. When its magnitude is non-zero, we observe that all the spins in the lattice tends to align themselves in its direction.

4.6.2 Phase change

Running the same procedure as the discrete case, we observe using the different measurables in our system that it is subject to a phase change at a critical temperature $T_C \approx 1.1$. As can be seen from the graphs in Figure 12, the drop in magnetization is not as strong as in the discrete case. Additionally, the plot of the magnetic susceptibility displays that the singularity occuring around T_C is less sharp and happens for temperatures slightly higher than the drop in magnetization.

4.6.3 Curie-Weiss law

Running the same procedure as above, we retrieve once again the inverse proportionality between the magnetic susceptibility and the temperature.(See Figure 13)

4.6.4 Hysteresis

We repeat the procedure explained in subsection 4.5. The graph obtained during this procedure can be seen below. We see once again that the history of the material is required to determine its state for a

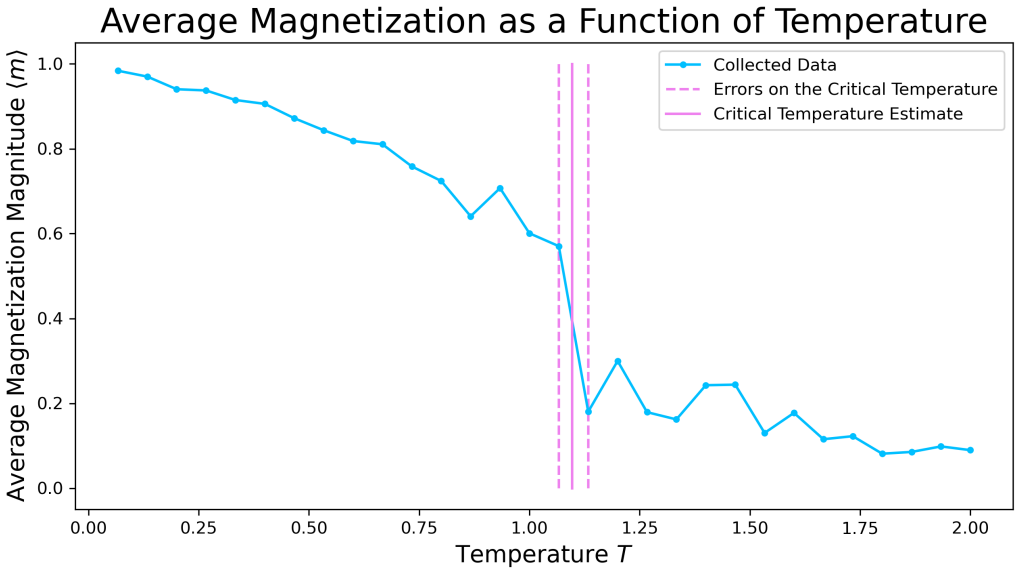

(a) $m - T$ diagram

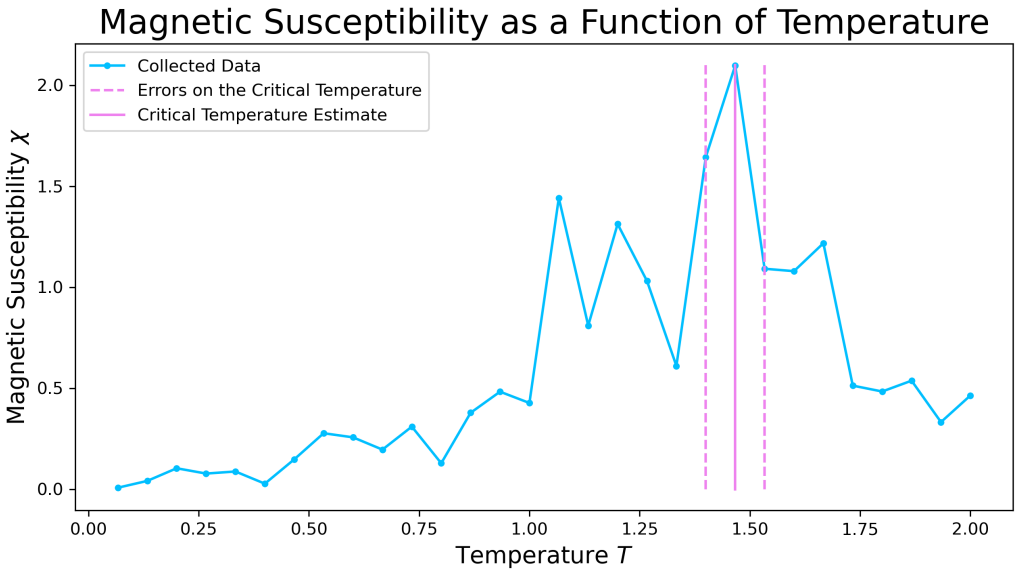

(b) $\chi - T$ diagram

Fig. 12: Plot of the different quantities in the continuous case for $L = 50$

given value of the magnetic field. Furthermore, we see that the magnitude needed for the magnetic field to trigger the change of magnetization is lower in the case of continuous spins compared to discrete ones.

4.6.5 Hypothesis

As seen above, we observe a critical temperature T_C much lower in the continuous case than in the discrete one. Let us try and present a possible hypothesis explaining that observation. We first recall that the critical temperature T_C is the temperature for which the material transitions from ferromagnetic to paramagnetic. The phase change arises from the thermal agitation of the atoms overtaking over the ferromagnetic interactions between neighboring moments. Now it is easy to surmise that in the continuous case, the interaction between neighboring spins is not as strong as for the discrete one. Indeed, for $\{\pm 1\}$ spins, the alignments is either perfect with the spins being parallel and the energy being minimized, or

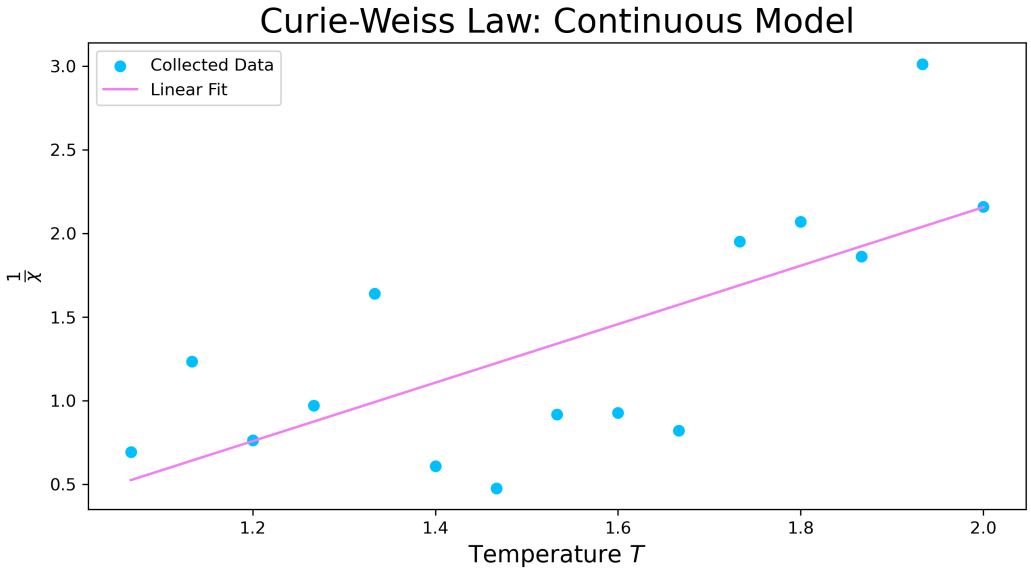

Fig. 13: Curie-Weiss law in the continuous case with $L = 50$

they are antiparallel. In the continuous case, however, we have every intermediate value, meaning that inside a Weiss domain, the interaction is not fully minimizing the energy (the spins are slightly misaligned). As such, the ferromagnetic effect is weaker and the domination of the thermal agitation appears earlier.

5 Conclusions

On the whole, the project has constituted a thorough exploration of the physics of phase transitions. Using a statistical physics framework and a finite, easily implemented 2D Ising model, we've been able to recover the Curie law as well as a quasi-singularity of the magnetic susceptibility around the critical point that is the Curie temperature and below which the susceptibility is no longer defined. This phenomenon goes hand in hand with spontaneous magnetization, a phenomenon explained by concepts from thermodynamics known as free energy and explicitly recoverable from the powerful partition function and the applications performed on it. It is very interesting to look at this project as an illustration of Helmholtz free energy and the effects of energy and entropy on configuration stability. An interesting continuation to this problem could be to analyze its analytic solution as a mathematical problem and explicitly recover the discontinuities of the free energy generating the phase transitions in question.

A final important note to make is contextualize the rigor of pour project as a demonstration of physics. We haven't proved the occurrence of anything in the real-world, but merely a good alignment of our simulation wit what is expected from the well-established postulates of statistical physics and thermodynamics. This can only serve as evidence that our model is a good experimentation environment that could serve as a quick way to pre-test hypotheses that we would like to later rigorously put to the test in a laboratory setting.

6 Contributions

The project has proven to be an exceptional demonstration of the efficiency of independent, asynchronous, and well-organized collaborative work. All authors were involved in the development of the basic simulation algorithms and Metropolis-Hasting protocols. Pillay and Mathiot were in charge of generating the essential data analysis used to demonstrate the results of this project as well as the simulation algorithms. Pillay was heavily involved in ensuring the integrity of all the data collection algorithms and further developed the code for the continuous version of the model. Mathiot was particularly involved in the description of the collected results and bringing them into the theoretical context. Sfeila was in

charge of establishing all the necessary theory and supporting knowledge regarding both the 2D Ising model as a mathematical problem as well as its specific meaning in the project's context, namely the Helmholtz free energy and its central role in dictating spontaneous process and the discontinuities of which correspond to the sought phase transitions. Sfeila was also in charge of the additional material regarding the simulation improvements by considering system autocorrelation and the convergence of the Markov chain's probability distribution to a stationary distribution.

A Appendix A: A Less Brief Introduction to the MCMC Method

The main problem with this probabilistic setup is the difficulty of computing the partition function at very large N - it involves a very large summation. It is important to outline the principles behind the simulation's methods in order to establish the robustness of the measurements performed; we want to show that the quantities measured indeed correspond to analogies of the physical quantities of interest in the framework of magnetic systems. Statistical physics draws the desired relation, and Monte-Carlo Markov Chain methods ensure we indeed measure what the partition function prompts us to measure.

A.1 Importance Sampling

Consider a function $f : J \subset \mathbb{R} \to \mathbb{R}$ defined on an interval J, and suppose we want to numerically and stochastically compute $I := \int_J f$. You might suggest uniform random variable sampling in the domain J and a function averaging over the length of the interval of definition. However, it can be shown that, from a convergence rate perspective, it is far more "rewarding" to gather information of f over regions where it is relatively large in absolute value. This motivates what is known as ¡b¿importance sampling¡/b¿. We can summarize this idea as:

$$I = \int_J f(x)dx = \int_J \frac{f(x)}{\rho(x)}\rho(x)dx \approx \frac{1}{N}\sum_{i=1}^{N} \frac{f(X_i)}{\rho(X_i)}$$

In the above expression, ρ is a probability density function that we use to incorporate importance sampling, and the family $(X_i)_i$ are realizations - or sampled results - of the continuous random variable defined by the probability density ρ. Indeed, as a consequence of the weak law of large numbers, we expect that the random variable defined by $\frac{1}{N}\sum_{i=1}^{N} \frac{f(X_i)}{\rho(X_i)}$ where the family $(X_i)_i$ is an identically distributed and independent family of random variables characterized by the PDF ρ will converge in probability to the expectation of $\frac{f(X_1)}{\rho(X_1)}$, which is shown to be the desired integral in the above expression. This is the spirit of stochastic integration. There are two important points to address:

- How do we choose ρ?
- How do we perform the $(X_i)_i$ sampling?

Based on the principle of importance sampling, we want the PDF to follow f. ($|f|$ to be more specific, but since our "difficult" integral here actually corresponds to the summation in the partition function, we can assume f to be nonnegative.) This prompts to take $\rho = f$, but we require ρ to be normalized, namely by the integral of f, which brings us back to the initial problem. However, we will see that, in the Metropolis-Hasting sampling algorithm, we avoid this problem by considering the relative values of the PDF. For now, we retain this notion of ρ following f.

A.2 Metropolis-Hasting - An Example of MCMC Algorithms

We tackle the sampling problem. The idea is to generate a ¡b¿ Markov Chain ¡/b¿:

$$x_1 \longrightarrow x_2 \longrightarrow x_3 \longrightarrow x_4 \longrightarrow ... \longrightarrow x_N$$

In the above "chain", the probability of sampling x at a given step is only dependent on the current step's state, not on previously achieved states (Markov chain property.) Hence, we can write:

$$P_{n+1}(x) = P_n(x)\,(1 - \sum_{y \neq x} W_{x \to y}) + \sum_{y \neq x} P_n(y) W_{y \to x}$$

In the above, $W_{x\to y}$ denotes the probability of a transition from x to y. It can be shown that, provided our transition probabilities ensure the ¡b¿ergodicity¡/b¿ of the chain (we will later show that our chains - in this project - are ergodic), the probability $(P_n)_n$ converges. We impose this sampling probability to be, at convergence, our ρ function, or the normalized f function. At convergence, we write $P_n + 1 \approx P_n \approx P$ and we obtain the balance equation:

$$P(x) \sum_{y \neq x} W_{x\to y} = \sum_{y \neq x} P(y) W_{y\to x}$$

And in our problem, this writes:

$$\rho(x)\, W_{x\to y} = \rho(y)\, W_{y\to x} \quad \forall x, y$$

In the Metropolis-Hasting algorithm, the transition probability of attaining y given that we are at x writes as a product $W_{x\to y} = T_{x\to y} A_{x\to y}$ where T is the probability of proposing the new state, and A is the probability of accepting it. It is very easy for us to choose proposed states and their probability of proposal T, and it is also easy to choose the proposing probability and the proposed states so that $T_{x\to y} = T_{y\to x}$ (say, if we flip one lattice state randomly and propose it in our problem.)

It is easily shown that taking $A_{x\to y} = \min\left(1, \dfrac{\rho(y) T_{y\to x}}{\rho(x) T_{x\to y}}\right)$ sastisfies the detailed balanced equation. Hence, we compute this acceptance rate and decide probabilistically whether to move to the new state. If we reject the change, we add the current state once again to the chain without change.

Observe that, by taking $\rho(y)/\rho(x)$, we can eliminate the need to compute the normalization factor of our probability function, which, in our case, was the tedious partition function!

Explicit function definitions are available in the `utils.py` script and in the appendices of this report. We can now generate Markov chains from our starting configurations by applying the Metropolis-Hasting algorithm and a given choice of a proposed change (see protocols in utils.py). Then, we can average any physical quantity over the configurations of the chain to obtain an average value of the given physical quantity such as magnetization for the system under the given conditions.

If we only propose states that have one toggled lattice site, many consecutive states will be correlated, and it will be irrelevant to measure the quantities in these states. This motivates the introduction of cycle lengths or a Monte Carlo time between measurements. This is what we call the autocorrelation time, which we dynamically implement and discuss more thoroughly in the report of this project. We also discuss the "warm-up time" which is necessary to ensure the convergence to a stationary distribution in the Markov chain.

B Appendix B: Computations

$$\begin{aligned}
\langle m \rangle = \frac{1}{\beta}\frac{\partial}{\partial J} \ln Z &= \frac{1}{\beta}\frac{\partial}{\partial J} \ln\left(\sum_{\sigma\in\{-1,1\}^N} e^{-\beta\,\mathcal{H}(\sigma)}\right) \\
&= \frac{1}{\beta}\frac{1}{Z} \sum_{\sigma\in\{-1,1\}^N} \beta \left(\sum_{i=1}^N \sigma_i\right) e^{-\beta\,\mathcal{H}(\sigma)} \\
&= \sum_{\sigma\in\{-1,1\}^N} \left(\sum_{i=1}^N \sigma_i\right) \frac{e^{-\beta\,\mathcal{H}(\sigma)}}{Z} \qquad (1) \\
&= \sum_{\sigma\in\{-1,1\}^N} \mathbb{P}(\sigma) \left(\sum_{i=1}^N \sigma_i\right) \\
&= \mathbb{E}\left[\sum_{i=1}^N \sigma_i\right]
\end{aligned}$$

$$
\begin{aligned}
\chi(T) = \frac{1}{N\beta}\frac{\partial^2}{\partial J^2}\ln Z = \frac{1}{N}\frac{\partial}{\partial J}\left(\sum_{\sigma\in\{-1,1\}^N}\left(\sum_{i=1}^N\sigma_i\right)\frac{e^{-\beta\,\mathcal{H}(\sigma)}}{Z}\right) \\
= \frac{1}{N}\sum_{\sigma\in\{1,-1\}^N}\left(\sum_{i=1}^N\sigma_i\right)\left(\beta\left(\sum_{i=1}^N\sigma_i\right)\frac{e^{-\beta\mathcal{H}(\sigma)}}{Z} - e^{-\beta\mathcal{H}(\sigma)}\left(\frac{1}{Z^2}\frac{\partial Z}{\partial J}\right)\right) \\
= \frac{\beta}{N}\left[\sum_{\sigma\in\{1,-1\}^N}\left(\sum_{i=1}^N\sigma_i\right)^2\mathbb{P}(\sigma)\right] - \frac{1}{N}\left[\frac{1}{Z}\frac{\partial Z}{\partial J}\sum_{\sigma\in\{1,-1\}^N}\left(\sum_{i=1}^N\sigma_i\right)\mathbb{P}(\sigma)\right] \\
= N\beta\,\mathbb{E}\left[\left(\frac{1}{N}\sum_{i=1}^N\sigma_i\right)^2\right] - \left(\mathbb{E}\left[\frac{1}{N}\sum_{i=1}^N\sigma_i\right]\right)^2 \\
= N\beta\,\mathrm{Var}\left[\frac{1}{N}\sum_{i=1}^N\sigma_i\right] \\
= N\beta\left(\langle m^2\rangle - \langle m\rangle^2\right)
\end{aligned}
\tag{2}
$$

$$
\begin{aligned}
\langle E\rangle = -\frac{\partial}{\partial\beta}\ln Z = -\frac{1}{Z}\sum_{\sigma\in\{1,-1\}^N} -\mathcal{H}(\sigma)e^{-\beta\mathcal{H}(\sigma)} \\
= \sum_{\sigma\in\{1,-1\}^N}\mathcal{H}(\sigma)\mathbb{P}(\sigma) \\
= \mathbb{E}[\mathcal{H}(\sigma)]
\end{aligned}
\tag{3}
$$

$$
\begin{aligned}
C_V(T) = \frac{\partial\langle E\rangle}{\partial t} = \frac{\partial}{\partial T}\left(\frac{1}{Z}\sum_{\sigma\in\{1,-1\}^N}\mathcal{H}(\sigma)e^{-\frac{1}{k_BT}\mathcal{H}(\sigma)}\right) \\
= \frac{1}{Z}\sum_{\sigma\in\{1,-1\}^N}\frac{\mathcal{H}(\sigma)^2}{k_BT^2}e^{-\beta\mathcal{H}(\sigma)} - \frac{1}{Z^2}\left(\sum_{\sigma\in\{1,-1\}^N}\mathcal{H}(\sigma)e^{-\beta\mathcal{H}(\sigma)}\right)\cdot\left(\sum_{\sigma\in\{1,-1\}^N}\frac{\mathcal{H}(\sigma)}{k_BT^2}e^{-\beta\mathcal{H}(\sigma)}\right) \\
= \frac{1}{k_BT^2}\left(\mathbb{E}[\mathcal{H}(\sigma)^2] - \mathbb{E}[\mathcal{H}(\sigma)]\right) \\
= \beta^2 k_B\ \mathrm{Var}\ [\mathcal{H}(\sigma)] \\
= \beta^2 k_B(\langle E^2\rangle - \langle E\rangle^2)
\end{aligned}
\tag{4}
$$

C Appendix C: Other Applications of the 2-Dimensional Ising Model

C.1 Lattice Gas Model

The lattice gas model is particularly useful in statistical mechanics for studying phase transitions, adsorption, and fluid behavior. The outline of this mathematical problem is tweaked to model this new statistical physics and condensed matter problem is as follows:

- A new interaction energy between gas atoms to replace the magnetic interaction term.
- A chemical potential term to replace the external field term.

Then, using the same Monte-Carlo steps redefined for this new Hamiltonian yields a similar stochastic integration and gives good insight into system characteristic behavior under different conditions. In particular, we can track:

– Phase Transitions: The lattice gas model can describe gas-liquid phase transitions, analogous to the magnetic phase transitions in the Ising model.

– Adsorption: The model helps in understanding adsorption phenomena, where particles adhere to surfaces or interfaces.

By leveraging the Ising model's well-developed theoretical framework, we can gain valuable insights into the behavior of lattice gases, making it a powerful tool in statistical mechanics.

C.2 Machine Learning and Neural Networks

The Ising model provides a powerful framework that allows us to better understand and interpret Hopfield networks and Boltzmann machines. This involves treating the neurons as lattice sites. As for the lattice gas model, adapting the Ising model to a new situation amounts to modifying the Hamiltonian function and reinterpreting the measurable quantities.

C.2.1 Hopfield Networks

The energy function of the Hopfield network is defined by:

$$E = -\frac{1}{2}\sum_{i \neq j} w_{ij} s_i s_j - \sum_i \theta_i s_i$$

In the above expression:

– w_{ij} are the weights between neurons i and j,
– s_i and s_j are the states of the neurons (usually +1 or -1),
– θ_i are the thresholds or biases for the neurons.

Observe that, unlike our project's model, this Hamiltonian features an infinite interaction range (assuming the weights are nonzero) rather than a nearest-neighbor interaction range; such modifications involve a deep analysis of the formalism of a given problem.

C.2.2 Boltzmann Machines

The energy function of the Boltzmann machine is defined by:

$$E(\mathbf{s}) = -\sum_{i<j} w_{ij} s_i s_j - \sum_i b_i s_i$$

In the above expression:

– w_{ij} are the weights between neurons i and j,
– s_i and s_j are the states of the neurons (usually 0 or 1),
– b_i are the biases for the neurons.

C.2.3 Applications of Hopfield networks and Boltzmann machines

– Pattern Recognition and Memory: In Hopfield networks, the Ising model helps in understanding how the network stores and retrieves patterns. Each stable state of the network corresponds to a stored pattern, similar to how spin configurations represent magnetic states in the Ising model.
– Learning Algorithms: Boltzmann machines use the Ising model's framework to define their learning algorithms. The gradient of the log-likelihood of data with respect to the weights involves expectations that resemble those in the Ising model.
– Optimization: The Ising model's principles are used in neural network optimization, where finding the optimal weights and configurations can be seen as finding the minimum energy state of the system.

D Appendix D: Further Discussion on the MCMC Algorithm

We tried not to get carried away by the numerical implementation and implications of our methods and algorithms as this is, at the end of the day, a physics project, and not a coding class. However, we dedicate this section to discussing methodology regarding using an MCMC approach and how we could theoretically enhance the accuracy of our results. We omit most of the information already presented at the beginning of this project to avoid redundancy.

D.1 Warm-up Time Incorporation in Dynamic Simulation

An important part of our MCMC method is the assumption of a stationary probability distribution for the Markov chain generation. States are characterized by their free energy, and since magnetization and free energy are related, we can confidently say that quasi-constant magnetization is a fine indicator of a stationary probability distribution. Hence, to compute optimal warm-up times - where optimal includes time-efficient and long enough - we can keep running metropolis moves until the magnetization stagnates using a stopping criterion. When working with fixed parameters, an interesting pipeline to create when running simulations would be to take input from the configuration and compute a warm-up time for these parameters by waiting for stagnation over a long enough period of Monte-Carlo time. Instead of computing a time on a copy of our configuration, we could even warm up our actual configuration until the magnetization stagnates if we are not keen on retaining the uninteresting initialization.

Even more interesting is the application of this approach to the dynamic case; if we misjudge the point of convergence before quickly reaching convergence, it is not a disaster. If, however, we decide to constantly change the system parameters such as the temperature of the applied field, the probability distribution changes at every change, and, in principle, we should halt measurements each time until the distribution has once again reached a stationary state. This translates to re-warming the system when subjected to parameter changes (recall that the probability distribution depends on the T and J dependent Hamiltonian as well as the T dependent β factor.

D.2 Autocorrelation

Another important part of the MCMC approach is the measurement process. With our main protocol (that which is used in most of if not all the simulations), we can only propose a small subset of the possible configurations starting from a given state; we propose the same state with one flipped spin only. Even though our system is ergodic, many consecutive states will be correlated, and a lot of irrelevant intermediate states may be crossed in the search for the equilibrium state of a system. We can measure the optimal cycle length - where optimal refers to as short as possible while separating decorrelated states efficiently - naively by computing the autocorrelation function at different at a given lag (Monte-Carlo time elapsed) k. States separated by this lag will be decorrelated if the autocorrelation function of the time series of the sampled states in question (at fixed parameters) is close to zero (i.e. it vanishes.) The autocorrelation function of a time series $(x_i)_{1\leq i\leq n}$ at a lag $k \in \{1, ..., n\}$ is given by:

$$\mathrm{ACF}(k) = \frac{\sum_{t=1}^{n-k}(x_t - \bar{x})(x_{t+k} - \bar{x})}{\sum_{t=1}^{n}(x_t - \bar{x})^2}$$

The autocorrelation time can then naively be computed by sampling a large enough time series and checking when the ACF is small enough (using a stopping criterion.) A big problem, of course, is that we may need to constantly resize our time series, but this isn't too bad since if we exceed the available lags, we can sample new states and only compute the new lag values without recomputing the old ones.

Typically, the autocorrelation function can be confidently said to decay exponentially with lag. This behavior, however, strongly fluctuates when nearing the critical temperature. Hence, this motivates a dynamic cycle length computing mechanism, which is easily implementable - as the warm-up time - by tweaking the animation generating function, namely its slider-activated function to include a cycle length computing based on configuration parameters which are readily fetched by the class methods.

Observe that the autocorrelation function typically scales as a decaying exponential of the lag, so a database of exponential factors would suffice to efficiently implement dynamic cycle length resizing in our simulations. Even better, the decay time can be computed in a database beforehand using these decaying factors (collected experimentally.) However, near the Curie temperature, this relation breaks. In fact, we have an interesting phenomenon displayed below and taken from opisthofulax's work on Physics StackExchange (not an academic source, but a very interesting result) depicted in Figure 14. As we can observe, the autocorrelation function decays much slower in close vicinity of the Curie temperature (Here, Onsager refers to the analytic solution of the Curie temperature in the framework of the author.)

D.3 Possible Improvements to MCMC Algorithm in Higher Computational Power Setting

Now, consider a project setting in which we had, at our disposal, an arbitrarily higher computational power, and where accuracy was arbitrarily more important than the time efficiency of our algorithms.

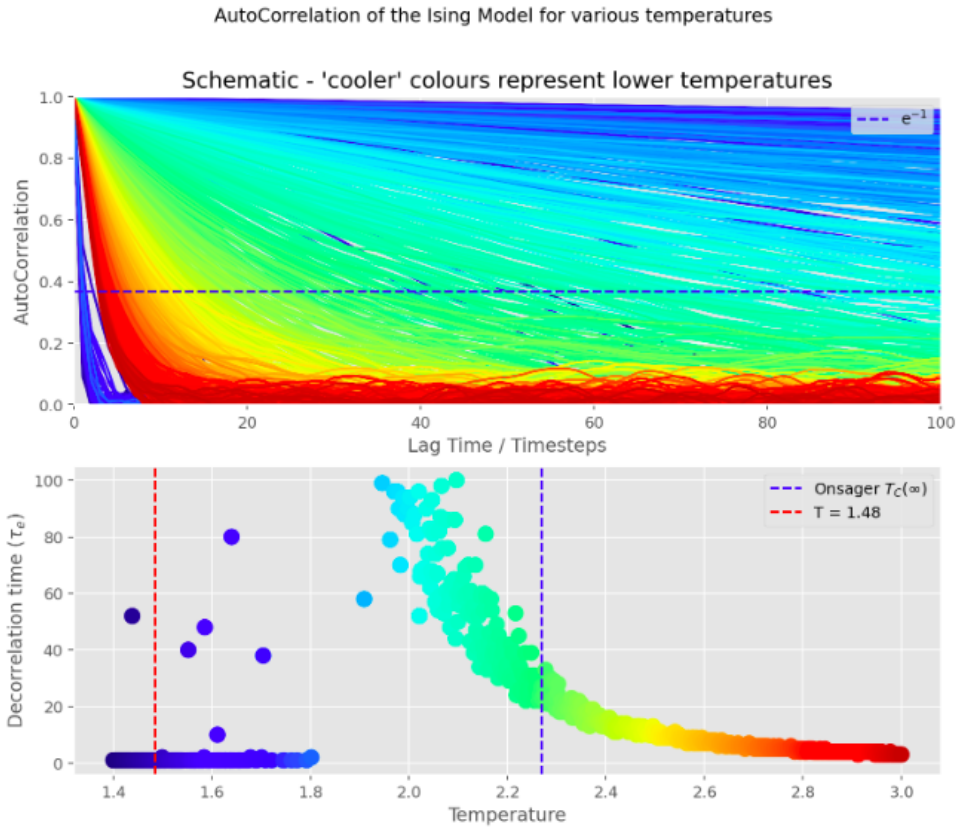

Fig. 14: ACF vs. Lagtime and Decorrelation Time vs. Temperature

Then, what we could do to improve the robustness of our Monte-Carlo simulations would be to incorporate the above notions into a simulation function that dynamically changes its Monte-Carlo parameters to accommodate changes to the temperature and applied external field. We do not implement this enhanced algorithm in Python as it is far too slow for our purposes and only marginally improves sampling, a trade-off we are not ready to make in our situation. It merely serves the purpose of discussion and raising further questions regarding simulation optimizations. Hypothetically, for optimal sampling and measurement accuracy, we would have to modify the slider activation functions of the temperature and external field strength to do the following:

- Upon change, halt measurements and begin tracking the magnetization of the system until it converges up to some stopping criterion.
- Once the system is warmed up, compute its autocorrelation time and adjust cycle length accordingly.
- Continue measurements.

We could tweak the simulation function to fetch cycle length and warm-up time as Configuration object attributes that are modified as the temperature and external field are changed. Moreover, rather than always computing these quantities in very frequented regions of parameters, we could, beforehand, create a database with the optimal value of these parameters, and replace computation upon slider movement with data fetching from databases in the directory.

Observe that the database approach is far more reasonable, because as we gain arbitrarily high computational power to the point where we can quickly compute warm-up time and cycle length, we may be nearing the computational power required to numerically compute the partition function and derive the quantities as the theoretical applications on this partition function, but this requires a numerical analysis of its own.

E Bibliography

References

1. Barry A. Cipra. "An Introduction to the Ising Model." *The American Mathematical Monthly*, vol. 94, no. 10, 1987, pp. 937–59. JSTOR, https://doi.org/10.2307/2322600. Accessed 30 May 2024.

2. Radzihovsky, Leo. "Physics 7240: Advanced Statistical Mechanics Lecture 2: Magnetism: Exact Solutions and Mean-Field Theories." Physicscourses.Colorado.Edu, Department of Physics, University of Colorado, Boulder, 28 Aug. 2019, https://physicscourses.colorado.edu/phys7240/phys7240_fa19/LectureNotesPhys7240F2019web/LectureSet2MagnetismMFT7240F2019.pdf. Accessed 31 May 2024.

3. Arnaud COUAIRON & Fabian CADIZ, *Classical Electrodynamics* (École Polytechnique, Palaiseau 2023) Chapter IX

4. V.L. Proud (https://physics.stackexchange.com/users/295029/v-l-proud), Decorrelation times for a 2D Ising Model over a range of temperatures, URL (version: 2023-02-07): https://physics.stackexchange.com/q/626649